Ab initio EPR parameters for dangling-bond defect complexes in silicon: Effect of Jahn-Teller distortion

Gernot Pfanner, Christoph Freysoldt, and Jörg Neugebauer
Max-Planck-Institut für Eisenforschung GmbH, D-40237 Düsseldorf, Germany

Uwe Gerstmann
Universität Paderborn, Lehrstuhl für Theoretische Physik, D-33098 Paderborn, Germany

(Received 3 February 2012; published 4 May 2012)

A dangling bond (db) is an important point defect in silicon. It is realized in crystalline silicon by defect complexes of the monovacancy V with impurities. In this work, we present spin-polarized density-functional theory calculations of EPR parameters (g and hyperfine tensors) within the GIPAW formalism for two kinds of db defect complexes. The first class characterizes chemically saturated db systems, where three of the four dangling bonds of the isolated vacancy are saturated by hydrogen (VH_3) or hydrogen and oxygen (hydrogen-oxygen complex, VOH). The second kind of db consists of systems with a Jahn-Teller distortion, where the vacancy includes either a substitutional phosphorus atom (the E center, VP) or a single hydrogen atom (VH). For all systems we obtain excellent agreement with available experimental data, and we are therefore able to quantify the effect of the Jahn-Teller distortion on the EPR parameters. Furthermore we study the influence of strain to obtain further insights into the structural and electronic characteristics of the considered defects.

DOI: 10.1103/PhysRevB.85.195202 PACS number(s): 61.72.J−, 76.30.−v, 71.15.Mb, 71.55.Cn

I. INTRODUCTION

The vacancy V is an important point defect in silicon, which originates from a missing atom in the host lattice, and which can form aggregates with further vacancies or with impurities. This is the case for oxygen, which is incorporated in Czochralski-grown silicon forming the well-known VO defect complex[1–3] (the A center) or, equivalently, with phosphorus forming the VP defect complex[4] (the E center). In addition, the interaction of vacancies with hydrogen has been of great interest,[5,6] since it can be used for a complete passivation of the vacancy.

One key experimental tool for the structural characterization of these defects is "electron paramagnetic resonance" (EPR) spectroscopy.[7–9] This extremely sensitive technique can yield information on the symmetry of the defect as well as on the chemical identity of the involved atoms. In the case of silicon, several hundreds of EPR centers have been reported so far.[10,11] From the spectrum one can obtain information on the g tensor (interaction of the unpaired spin with the external magnetic field) and the (super-) hyperfine tensors A (interaction of the unpaired spin with the spins of nuclei nearby). Both are characterized by their eigensystem, i.e., their eigenvectors and eigenvalues, but it is also common usage to express A through a set of (hyperfine) parameters,[9] namely the Fermi contact interaction a, the uniaxiality b, and the rhombicity c.

From experimental data alone, in particular from the relative intensities of the hyperfine satellite line to the central lines, one obtains information about the atomic species involved in the defect structure. However, the development of a detailed atomistic structural defect model requires comparison with theoretical calculations of the EPR parameters. A very efficient approach for defects in semiconductors is based on spin-dependent "density functional theory" (DFT) utilizing *ab initio* pseudopotentials.[12,13] In particular, the computation of the g tensor is conceptually challenging and a proper method for the plane-waves basis set has been established only recently (GIPAW-formalism).[12]

With such an accurate method at hand, it is possible to study, for example, how the symmetry-lowering Jahn-Teller (JT) distortion of point defects in silicon is related to the measured EPR parameters. In this material essentially three kinds of JT-distorted systems have been studied so far, namely the already mentioned monovacancy,[8,14] the E center,[4,15,16] and the divacancy.[17–20] For the E center and the divacancy, there has been a long debate concerning the true symmetry-lowering relaxation mode of the ground state, which can be either resonant or pairing.[21,22] In the case of the pairing JT distortion, two defect neighbors form a long Si-Si bond, so that the distance between these atoms d_1 becomes smaller than their common distance to the third neighbor d_2 (i.e., $d_1 < d_2$). The resonant JT-relaxation mode corresponds to the opposite case: Two atoms move apart while the third neighbor moves toward both atoms, so that finally there are two shorter distances and a larger one (i.e., $d_1 > d_2$). As *ab initio* calculations have shown, both configurations have a similar formation energy and have consequently a comparable stability.[21,23–25]

In this work, we present spin-polarized DFT calculations of the EPR parameters for two kinds of db defects in crystalline silicon (see Fig. 1). The first kind has only one unpaired electron inside the vacancy with the other three electrons chemically bonded to impurities. One of these models originates from the A center, i.e., the oxygen-vacancy complex, if an additional hydrogen is trapped inside the defect (VOH). The other one is the hydrogenated vacancy with three hydrogens attached (VH_3), which has been identified by Fourier transform infrared[26–28] and Raman[29,30] spectroscopy but not by EPR so far. The second class of db models has initially three unpaired electrons inside the vacancy, so that the structure undergoes a symmetry-lowering JT distortion upon relaxation. Specifically we consider the E center with a substitutional phosphorus (VP) and the vacancy containing a

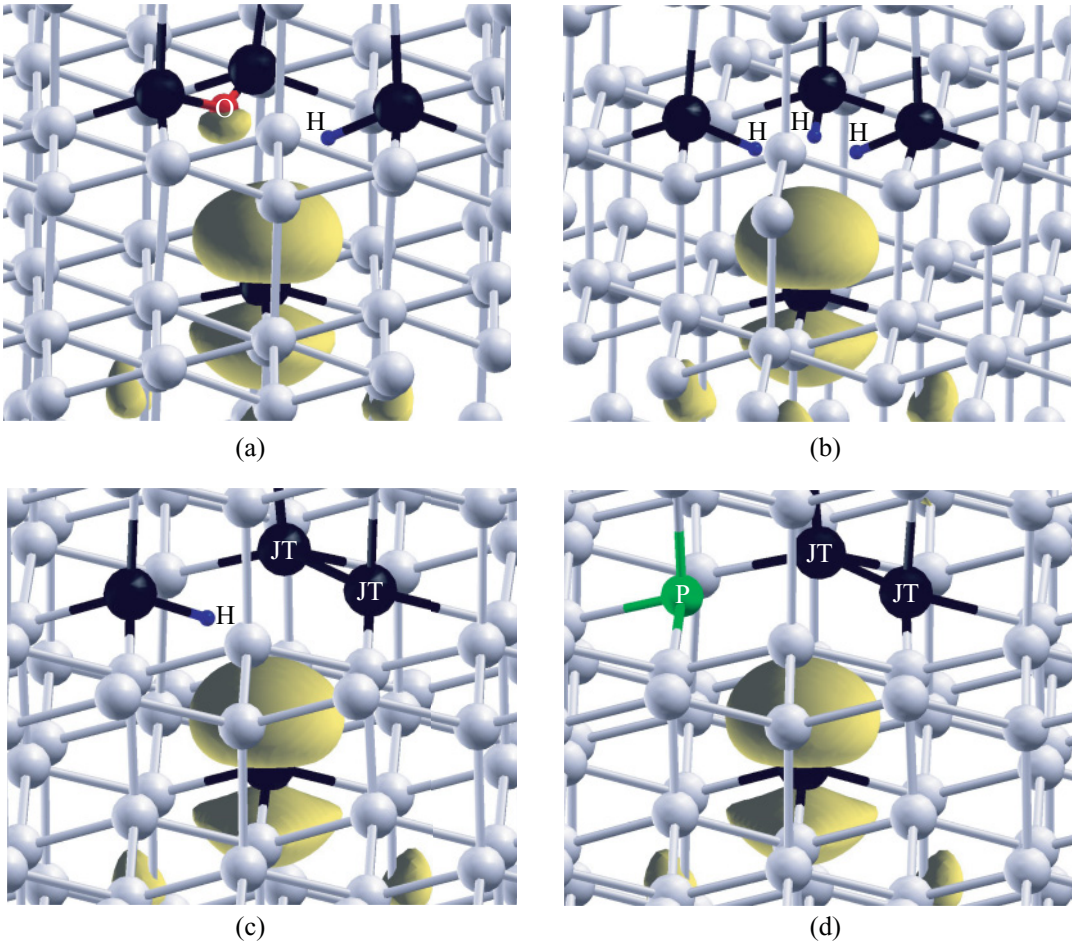

FIG. 1. (Color online) (a): The VOH db model: oxygen (red color) binds to two neighbors (black color) of the vacancy. The hydrogen atom (in blue) passivates the broken bond of the third neighbor, leaving one unpaired electron, which is located on the fourth neighbor of the vacancy (as indicated by the spin density in yellow). Notably there is also spin polarization on the oxygen atom. (b): The VH_3 db model: three hydrogen atoms passivate the corresponding broken bonds of the vacancy. (c): The VH db model: Two neighbors (JT) of the vacancy form a long bond, whereas the third is again passivated by hydrogen. (d): VP db model: Again two silicon atoms (JT) combine. Substitutional phosphorus (green color) removes the third electron from the vacancy.

single hydrogen (VH). From the comparison of both db-defect classes we show the actual impact of the JT distortion on the EPR parameters. For further characterization of the db systems, we consider the influence of hydrostatic strain. This conceptual study gives us trends which are useful for the interpretation of EPR data in hydrogenated amorphous silicon.[31–33]

II. COMPUTATIONAL METHODS

For the *ab initio* calculation of the EPR parameters, we have used the plane-wave DFT code QUANTUM ESPRESSO[34] (v4.2.1), in which the GIPAW formalism[12] has been recently implemented. We employ the Perdew-Burke-Ernzerhof functional[35] and norm-conserving pseudopotentials[36] with a scalar-relativistic correction for silicon.[8,37] Convergence of the relaxation and EPR parameters with respect to the plane-wave cutoff is found to be within 30 Ry. Notably, within this approach one does not observe a strong dependence of the isotropic hyperfine coupling on the cutoff energy as found previously for the single-projector approach.[13,38] Our initial structures reflect the perfect D_{3d} defect symmetry, and in particular, we do not place any symmetry constraints on the expected JT distortion for the VH and VP db model. The maximum force on an atom is below 4 meV/Å, which is adequate for getting the characteristics of the db models. The Brillouin zone integration is done on a Monkhorst-Pack mesh.[39] The geometric relaxation and the hyperfine parameters can be obtained with sufficient accuracy by a $3 \times 3 \times 3$ sampling. The computation of the g tensor requires a significantly denser $6 \times 6 \times 6$ **k**-point mesh.

The db models are based on a supercell approach. To compare with experiment we use $3 \times 3 \times 3$ cells (216 Si atoms without the defect), which also gives us the possibility to study the distribution of the spin into the further network. For obtaining the relevant dependencies of the EPR parameters on strain, we relax the system at different lattice constants. In the case of the strained VOH and VH_3 db models, we make use of smaller, less resources-demanding $2 \times 2 \times 2$ supercells (64 atoms without the defect), since their electronic structure is less sensitive to the supercell size. To circumvent the already-mentioned problems with the mode of JT distortion for the VH and VP db model, i.e., pairing or resonant, we start the

relaxation for strained cells from the relaxed, pairing-distorted structure at the ideal lattice constant. This procedure ensures the stability of the pairing relaxation mode under study (i.e., the localized db character) for a broader range of applied strain.

For comparison of our results with an all-electron approach,[40] we have carried out calculations for small molecular radicals. In accordance with previous studies,[41] we consider the silyl (SiH_3) and tetrasilyl radical (Si_4H_9), for which we take the structure from the all-electron calculation to remove the effects of differences in the local db geometry. We employ an uncontracted WTBS basis set for silicon and the EPR-III basis set for hydrogen, and a Douglas-Kroll-Hess 0-order relativistic Hamiltonian. For the uniaxial g tensor we obtain a discrepancy on the order of 0.001 for the normal component and a negligible difference for the parallel component. The isotropic hyperfine constant of the db atom shows a significant deviation for the silyl radical (on the order of 120 MHz, i.e., 19%), which can be attributed partly to core-polarization effects. This is also indicated by the much smaller disagreement for the tetrasilyl radical (on the order of 40 MHz, i.e., 13%). In contrast to that, the anisotropic coupling constant is practically the same in both approaches. The isotropic couplings for the hydrogen atoms are more sensitive, which can be related to the polarization by the spin density of the db atom. The differences are smaller for weakly-polarized hydrogen (∼3 MHz). The results for our crystalline dangling bonds are not so strongly affected by this discrepancy, since the hydrogen atoms in these systems have a small coupling to the spin density as well.

III. RESULTS AND DISCUSSION

A. Defect geometry

The relaxation pattern strongly depends on the chemical composition of the defect complex. In the case of VOH the two silicon atoms bonded to the oxygen move into the vacancy, while in turn, the db atom and the neighbor with the attached hydrogen move outwards. The resulting defect symmetry is C_{1h} in accordance with previous findings.[42,43] In comparison to bulk silicon, the bond lengths of the db atom to its next neighbors are shorter whereas the corresponding bond angles are larger, which essentially means that the db atom is pressed into the network. Such a tendency can be also seen for the VH_3 db model, for which actually all defect neighbors move away from each other due to the small space in the vacancy. In this case, the relaxed defect symmetry is C_{3v}, and the db geometry is again rather planar. For the VH and the VP model one obtains the experimentally observed[15] defect symmetry (C_{1h} symmetry) as well as the formation of a long Si-Si bond with a length of 3.08 Å and 2.95 Å, respectively. The relaxation corresponds in both cases to a pairing JT distortion with the larger defect-neighbor distance being 3.67 Å and 3.59 Å, respectively. The db atom remains essentially at the bulk lattice site. However, whereas the SiH group of VH moves outwards, the phosphorus atom of the VP db model relaxes toward the defect center. The db geometry of both models is not uniform with respect to the backbond neighbors, but on average the angles are smaller compared to the VOH and VH_3 model. This is also reflected in the hyperfine parameters as we will discuss below.

We note in passing that the relaxation pattern is rather insensitive to the computational details. At first glance, this is surprising, since the modeling of the monovacancy shows the opposite tendency.[1,21,44,45] Apparently the presence of an impurity stabilizes the JT distortion.

B. The effect of the Jahn-Teller distortion on the EPR parameters

In Table I we compare the results of our DFT calculations with experimental data for the g tensor. The overall agreement is on the same order as the above-mentioned methodological differences between the GIPAW and the all-electron calculation for small molecular systems. In general, the theoretical eigenvalues tend to underestimate the experimental ones, and

TABLE I. Comparison of *ab initio* calculations with experiment for the g tensor for various deep-level defects in crystalline silicon. The isotropic component is denoted by g_{Iso}, and g_X, g_Y, g_Z stand for the eigenvalues associated with the corresponding principle axis. Θ is the angle between g_Z and the [110] axis.

		VOH	VH_3	VH	VP
g_{Iso}	Theory	2.0059	2.0074	2.0060	2.0068
	Exp. (Refs. 4,15, and 43)	2.0061		2.0070	2.0071
	Δ	− 0.0002		− 0.0010	− 0.0003
g_X	Theory	2.0082	2.0108	2.0121	2.0128
	Exp. (Refs. 4,15, and 43)	2.0086		2.0114	2.0112
	Δ	− 0.0004		0.0007	0.0016
g_Y	Theory	2.0081	2.0108	2.0063	2.0079
	Exp. (Refs. 4,15, and 43)	2.0084		2.0090	2.0096
	Δ	− 0.0003		− 0.0027	− 0.0017
g_Z	Theory	2.0013	2.0005	1.9995	1.9996
	exp. (Refs. 4,15, and 43)	2.0013		2.0006	2.0005
	Δ	0		− 0.0011	− 0.0009
Θ	Theory	39.1°	35.3 °	27.2°	30.6°
	Exp. (Refs. 4,15, and 43)	39.2°		32.4°	32°
	Δ	− 0.1°		− 5.2°	− 1.4°

TABLE II. Comparison of *ab initio* calculations with experiment for the A tensor for various deep-level defects in crystalline silicon. a stands for the isotropic, and b for the anisotropic hyperfine parameter, respectively. In addition to that, the eigenvalues of the A tensor, A_X, A_Y, A_Z, are reported. Θ is the angle between A_Z and the [110] axis. The difference between experiment and theory is given by Δ. For completeness we also mention the results from a self-consistent, semiempirical tight-binding (tb) calculation[47] for the hydrogen-vacancy db defects.

		VOH	VH_3	VH	VP
a (MHz)	Theory	− 292	− 314	− 337	− 350
	Exp. (Refs. 4,15, and 43)	− 297		− 328	− 347
	Δ	5 (2%)		− 9 (3%)	− 3 (1%)
	Theory (Ref. 47) (tb)		− 498	− 457, − 464	
b (MHz)	Theory	− 61	− 60	− 52	− 52
	Exp. (Refs. 4,15, and 43)	− 61		− 53	− 52
	Δ	0		1 (3%)	0
	Theory (Ref. 47) (tb)		− 56	− 47, − 44	
A_X (MHz)	Theory	− 230	− 253	− 285	− 300
	Exp. (Refs. 4,15, and 43)	− 236		− 275	− 295
A_Y (MHz)	Theory	− 231	− 253	− 285	− 300
	Exp. (Refs. 4,15, and 43)	− 236		− 275	− 295
A_Z (MHz)	Theory	− 414	− 434	− 442	− 451
	Exp. (Refs. 4,15, and 43)	− 418		− 435	− 450
Θ	Theory	34.7°	35.3°	35.4°	35.4°
	Exp. (Refs. 4,15, and 43)	35.3°		35.3°	35.3°
	Δ	− 0.6° (2%)		0.1° (0%)	− 0.1° (0%)
	Theory (Ref. 47) (tb)		35.3°	35.3°, 35.5°	

the differences are slightly larger for the systems with a JT distortion. The angle Θ between Z and the [110] axis shows a negligible deviation for the VOH defect and a large one for the VH defect. The g_{Iso} value has a smaller variation among different db defects compared to surface db defects.[46] Besides this one can clearly see how the JT distortion affects the g tensor. Firstly, it breaks the uniaxial symmetry observed for the VOH and VH_3 model. This is intuitively clear, since the bonding state lowers the electronic symmetry, which is crucial for the g tensor.[8,9] Secondly, the Z axis is oriented differently for the JT-distorted systems, since Θ is larger than the ideal value (35.3°) for the VOH model but smaller for the VH and VP defect.

The calculated hyperfine tensor agrees very well with experiment (see Table II) with an error on the order of 10 MHz for the isotropic coupling and a practically vanishing one for the anisotropic coupling. The larger discrepancy for the a parameter is expected, since this quantity depends on the spin density $\rho(r)$ close to the nucleus,[8,37] whereas the b parameter is an integrated quantity.[8,13] Consequently, the isotropic parameter should also be more sensitive to differences in $\rho(r)$. Interestingly, the agreement between theory and experiment is much better than expected from the pure theoretical error bar derived from our molecular test systems. We attribute this to a less pronounced effect of core polarization in the crystalline environment, since the spin density is able to delocalize into the network and it is consequently smaller in magnitude at the db atom. The variation in the hyperfine parameters among the considered models is larger than for the surfaces,[46] which can be explained by the larger variations in the db geometry as well as the effect of the long Si-Si bond. The a parameter indicates the s character of the wave function,[13] which in turn is related to the bond angle (Fig. 2). As visible, the coupling becomes smaller with increasing bond angle (between the db atom and the backbond atoms) which agrees with the sp hybridization picture of the db orbital.[41] However, one does not observe a corresponding increase in the b parameter (which probes for the p character in sp bonded systems like silicon), since this quantity is more affected by the long Si-Si bond in the JT-distorted systems (Table II) as expected from its stronger spatial dependence on the defect surrounding compared to a. It is interesting to note that the JT distortion has no affect on the symmetry and the orientation of the A tensor. Overall these findings clearly show that the g tensor is sensitive to the electronic structure beyond the spin-carrying db orbital, and the hyperfine tensor to the local spin-density distribution, respectively.

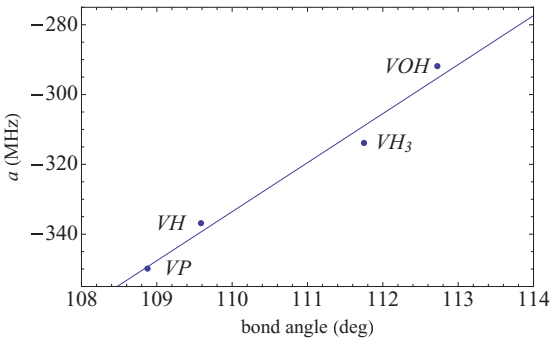

FIG. 2. (Color online) The relation between the isotropic hyperfine constant and the mean bond angle between the db atom and its backbond neighbors. The trend follows the expectation of sp hybridization of the db orbital (Ref. 41). The bond lengths among the db models vary insignificantly (on the order of 0.02 Å).

TABLE III. Isotropic superhyperfine couplings (in MHz) for characteristic defect atoms. The number of occurrences is denoted in brackets. Si (JT) stands for the silicon atoms forming the long Si-Si bond, and Si (JT-bb) stands for a corresponding neighbor (one per each involved Si atom), Si (H) for the silicon atom bond to hydrogen, and Si (2nd-bb) and Si (3rd-bb) denotes the second and third backbond neighbor of the db atom respectively.

Atom	VOH	VH_3	VH	VP
Si (JT)			–40 (2×)	–40, –42
Si (JT-bb)			–24 (2×)	–28 (2×)
Si (H)	–25	–11, –12 (2×)	–4	
Si (2nd-bb)	–31, –35 (2×)	–35 (3×)	–29, –32 (2×)	–29, –31 (2×)
Si (3rd-bb)	–21 (3×)	–17, –18 (2×)	–14, –15 (2×)	–13, –14 (2×)

It is also illuminating to consider the superhyperfine coupling of neighbors because it gives a better understanding of the spin distribution within the network. For that purpose we list the isotropic hyperfine couplings of relevant Si atoms in Table III (see also Fig. 3). First, we recognize that the net coupling between the atoms forming the weak bond is almost the same for the VH and the VP model. The rather small value agrees well with the expectation of a long Si-Si bond between both atoms. Furthermore, for the VP defect, there is again excellent agreement with the experimental value,[4] $a_{\mathrm{Exp}} = 37$ MHz, with the difference thus being only 5 MHz. This again proves that we are able to reproduce the measured defect geometry unambiguously. From the results it is also obvious that some spin leaks out into the local environment of the weak Si-Si bond, since each atom has one neighbor with a significant isotropic coupling. Besides these effects specific to the VH and VP model, one obtains in general a strong superhyperfine coupling on the second backbond neighbor of the db atom, which has been already observed in previous studies.[41,46] For the VH model, the deviation from experiment[48] is again rather small (3 MHz). Overall, the isotropic coupling at the backbond atoms is determined by the bond angle at the db atoms. The larger the bond angle (see Fig. 2), the larger the isotropic hyperfine coupling at the backbonds. This observation is in agreement with the expectation that for large bond angles more spin density is pressed into the network.

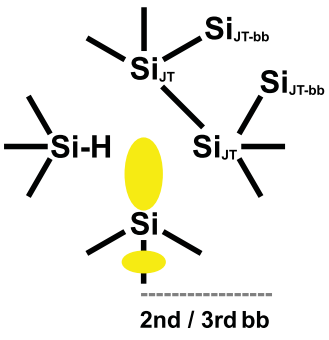

FIG. 3. (Color online) Illustration of the characteristic defect atoms for the VH defect. Two vacancy neighbors [Si (JT)] form a long Si-Si bond. Each bond partner has one backbond neighbor with a significant isotropic hyperfine coupling [Si (JT-bb)]. One vacancy neighbor is passivated by hydrogen [Si (H)]. Further characteristic atoms are located at the backbond side of the dangling bond [Si (2nd-bb), Si (3rd-bb)]. The corresponding hyperfine parameters for the considered db models are listed in Table III.

For completeness we mention that the hyperfine parameters for the hydrogen and the phosphorus atom are also close to their experimental counterparts. In case of hydrogen it is important to use a functional based on the general gradient approximation[38] to obtain a reasonable isotropic coupling constant.[49] For the VOH defect (the only model with a significant a coupling) it then differs by 1 MHz from the experimental value,[43] whereas the b parameter shows a discrepancy of about 0.6 MHz. The hyperfine interaction of the phosphorus atom is also reproduced[4] well by theory (the difference is practically vanishing).

Concerning the relative orientation of the g and A tensor, it is interesting to note that they are perfectly aligned (i.e., the angle α between g_Z and A_Z is zero) only for the VH_3 defect with the C_{3v} symmetry. For the VOH and the VP defect with the C_{1h} symmetry, both tensors have slightly different orientations with α being 4.45° and 4.80° respectively. The VH dangling bond has an even larger angle ($\alpha = 8.22°$). In particular the deviation for the VOH defect is remarkable, since it shows that collinearity is not always fulfilled when both tensors are uniaxial.

C. Strain

We have also considered the dependence of the EPR parameters on hydrostatic strain, since this can give further insights into the structural characteristics of the db defect. For large compressive strain (2–5% of the lattice constant x_0), the band gap closes and the system becomes metallic. In this case, the JT distortion changes to a resonant mode, since the spatial separation of the unpaired electrons becomes smaller and their interaction is enhanced. For very large tensile strain (more than 5% of x_0), the distances among the silicon defect neighbors become similar (i.e., $d_1 = d_2$) and, consequently, the JT distortion vanishes. In conclusion, since we are only interested here in the db character of the VP and VH defect, we only consider a parameter range in which the db character is preserved and for which the JT distortion corresponds to a pairing mode.

Figure 4 shows the trends for the principal values of the g tensor under strain. We see that $g_{X/Y}$ decreases with increasing lattice constant, as expected from the second-order perturbation picture,[8,9] according to which the deviation from the free-electron value is inversely proportional to the energy splitting between the singly-occupied db orbital and all other orbitals. Our results illustrate in particular that for large tensile strain, the specific chemical environment becomes

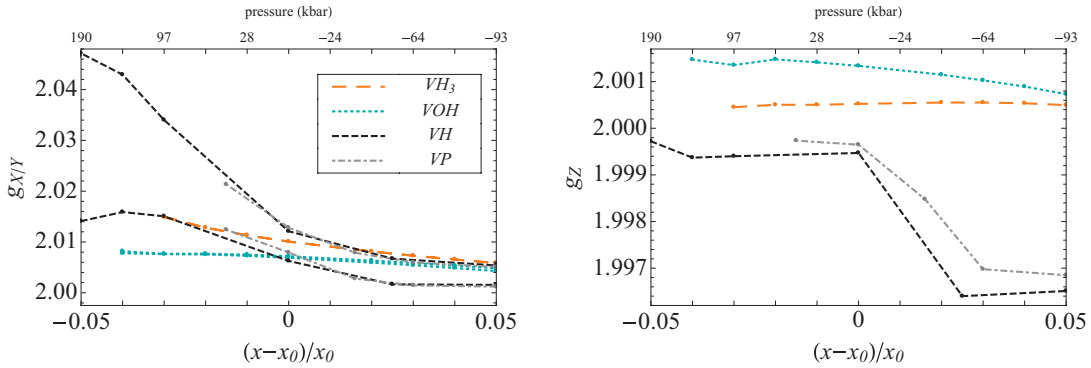

FIG. 4. (Color online) The variation of the principal values of the g tensor with respect to strain, characterized by the deviation from the lattice constant x_0. For compressive strain we only consider the range in which the db character of the system is preserved. (VH_3: large-dashed, orange line; VOH: dotted, cyan line; VH: dashed, black line; VP: dot-dashed gray line).

insignificant, since both the VOH and the VH_3 model converge to the same g values. The JT-distorted systems have a significantly deeper decrease for g_X and g_Y, whereas the g_Z components are more or less just shifted with respect to the other two db systems. Besides that, compressive strain leads to a larger rhombicity, which might originate from the electronic coupling to a larger number of orbitals as the band gap closes.

For the hyperfine parameters we observe the following trends for the VOH and the VH_3 model (Fig. 5). The isotropic coupling decreases with increasing lattice parameter, while the anisotropic coupling increases at the same time. This can be attributed to the sp hybridization of the db orbital, and it is in accordance with previous findings.[41] As shown in Fig. 6, the bond length becomes gradually larger the more the lattice is stretched. At the same time, the system relaxes to a more planar structure with larger bond angles. Consequently, the db orbital changes from an sp^3 configuration to a pure p one, and this then leads to the observed hyperfine parameters with increased anisotropic parts b.

The JT-distorted db systems have in principle a similar dependence of the bond parameters on strain. In particular, the bond lengths scale similarly as for the nondistorted defects. The larger deviations in the bond angles for compressive strain can be traced back to the asymmetry in the db structure (one angle is smaller than the other two), and it decreases for larger lattice constants. A similar trend is found for the anisotropic coupling, namely the b values for the VP and VH model are shifted upward by about 10 MHz compared to the VOH and VH_3 defect. However, for the a parameter the most significant difference between the JT and the nondistorted db systems is observed for tensile strain up to 5%. This can be related to the spin coupling of the unpaired db electron with the electrons forming the long Si-Si bond, since their isotropic hyperfine coupling increases in this range. It can also be seen in the distances between the defect neighbors, for which the difference between d_1 and d_2 (i.e., the structural characteristics of the JT distortion) becomes gradually smaller with increasing tensile strain. For larger lattice constants, the JT-distorted systems also show the effect of sp hybridization. This picture is also consistent with the observations made for the g tensor, i.e., that for large tensile strain, the db defect is basically determined by the local (planar) structure and not by electronic effects. In summary, the influence of strain on the EPR parameters is characterized by the band gap for compressive strain, and by the bond angle for large tensile strain. While the qualitative effects have already been discussed in the context of hydrogenated amorphous silicon,[32,50] our studies show that variations of strain on the order of 0.01 have a noticeable influence (such as 10–20 MHz for the isotropic hyperfine coupling).

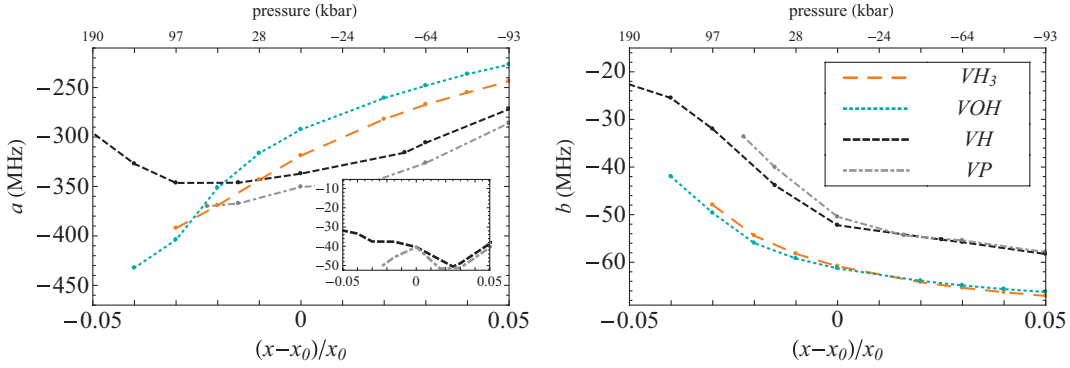

FIG. 5. (Color online) The variation of the hyperfine parameters with respect to strain, characterized by the deviation from the lattice constant x_0. For compressive strain we only consider the range in which the db character of the system is preserved. The inset in the left figure shows the corresponding dependence of the defect neighbors Si (JT) which form the long Si-Si bond. (VH_3: large-dashed, orange line; VOH: dotted, cyan line; VH: dashed, black line; VP: dot-dashed gray line).

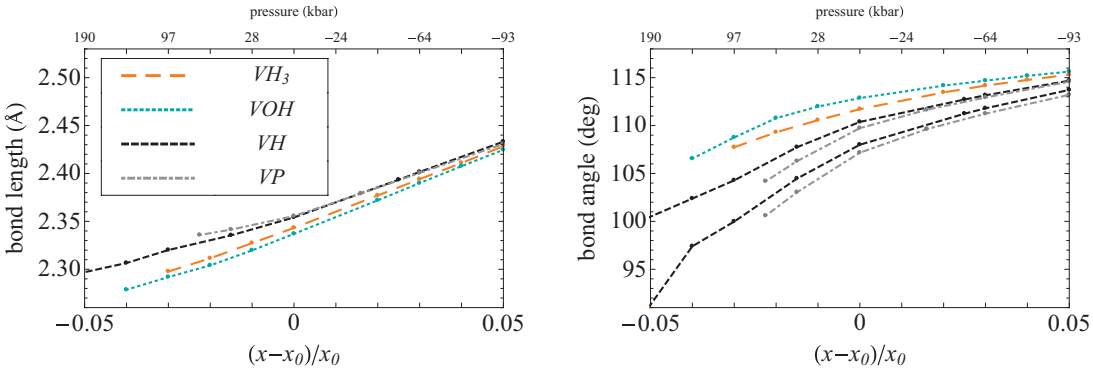

FIG. 6. (Color online) The variation of the bond parameters (bond length and bond angle) at the db atom with respect to strain characterized by the deviation from the lattice constant x_0. For compressive strain we only consider the range in which the db character of the system is preserved. The three bond lengths for the VH and VP model are approximately equal (within 0.02 Å). However, since one bond angle is notably smaller than the other two, we plot it separately in the figure on the right side. (VH_3: large-dashed, orange line; VOH: dotted, cyan line; VH: dashed, black line; VP: dot-dashed gray line).

IV. CONCLUSIONS

In this article we have considered four prototypical dangling-bond models in crystalline silicon. Two models are based on a complete passivation of the remaining three defect electrons either by hydrogen and oxygen or instead by three hydrogens. The other two models contained either a substitutional phosphorus (the E center) or a single hydrogen trapped inside the vacancy.

From our results we conclude that there is good agreement between the available experimental data and our theoretical approach (GIPAW formalism). On the one hand, this implies that we have found the experimentally relevant atomic structures, in particular confirming the expectation of a pairing Jahn-Teller distortion in case of the VP and VH defect.[4,15] Notably, the difficulties in the theoretical modeling of the monovacancy do not occur.[1,21,44,45] On the other hand, our results also quantify the accuracy of the GIPAW formalism for point defects in silicon, which is on the order of a few thousandths for the g tensor and up to 3% for the hyperfine parameters.

Furthermore we have shown how the JT distortion affects the EPR parameters. For these models, the g tensor becomes rhombic and the angle between the Z component and the [110] direction is smaller than the ideal one. In the hyperfine parameters, the JT distortion causes a smaller anisotropic hyperfine coupling (i.e., smaller p character of the db orbital). On the other hand, the isotropic hyperfine coupling of all db models can be explained by the bond angle of the db atom. With respect to db defects in hydrogenated amorphous silicon,[31] it is interesting to note that the isotropic hyperfine parameter shows only a small variation (in between 290–350 MHz) among the considered crystalline db models.

A systematic decrease of the isotropic coupling can be observed for large tensile strain, when the db models become planar independently from their actual electronic structure. For compressive strain, the main influence is given by the band gap, i.e., the amount of strain (on the order of 2–5% of the lattice constant x_0) for which the unpaired electron delocalizes and the system thus becomes metallic. For the mode of the JT distortion this implies that one observes the resonant mode for compressive strain and the pairing distortion for tensile strain respectively.

ACKNOWLEDGMENTS

This work was supported by the German ministry of Research and Education in the BMBF research project "EPR-Solar" (03SF0328F), and we are greatly indebted to K. Lips, A. Schnegg, and M. Fehr for fruitful discussions. Furthermore we want to thank A. Duff for proofreading the manuscript.

[1] D. Drabold and S. Estreicher, editors, *Theory of Defects in Semiconductors*, Vol. 104 of *Topics in Applied Physics* (Springer, Berlin, 2007).
[2] R. C. Newman, J. Phys.: Condens. Matter **12**, R335(2000).
[3] G. D. Watkins and J. W. Corbett, Phys. Rev. B **121**, 1001 (1961).
[4] G. D. Watkins and J. W. Corbett, Phys. Rev. **134**, A1359 (1964).
[5] S. Estreicher, Mater. Sci. Eng., R **14**, 319 (1995).
[6] A. L. S. Ferreira-Resende, Ph.D. thesis, University of Exeter (1999).
[7] M. Kaupp, M. Bühl, and V. G. Malkin, *Calculation of NMR and EPR parameters* (Wiley, Weinheim, 2004).
[8] J. M. Spaeth and H. Overhof, *Point defects in semiconductors and insulators* (Springer, Berlin, 2003).
[9] J. A. Weil and J. R. Bolton, *Electron paramagetic resonance* (Wiley, New Jersey, 2007).
[10] O. Madelung, U. Rössler, and M. Schulz, editors, *Silicon, paramagnetic centers, general remarks*, Vol. 41A2a of *Landolt-Börnstein - Group III Condensed Matter* (SpringerMaterials, Berlin, 2002).
[11] T. Umeda, Physica B **376**, 249 (2006).
[12] C. J. Pickard and F. Mauri, Phys. Rev. Lett. **88**, 086403 (2002).
[13] C. G. Van de Walle and P. E. Blöchl, Phys. Rev. B **47**, 4244 (1993).

[14]M. Sprenger, S. H. Muller, E. G. Sieverts, and C. A. J. Ammerlaan, Phys. Rev. B **35**, 1566 (1987).
[15]B. B. Nielsen, P. Johannesen, P. Stallinga, K. B. Nielsen, and J. R. Byberg, Phys. Rev. Lett. **79**, 1507 (1997).
[16]S. Öğüt and J. R. Chelikowsky, Phys. Rev. Lett. **91**, 235503, (2003).
[17]J. G. de Wit, E. G. Sieverts, and C. A. J. Ammerlaan, Phys. Rev. B **14**, 3494 (1976).
[18]S. Öğüt and J. R. Chelikowsky, Phys. Rev. Lett. **83**, 3852 (1999).
[19]E. G. Sieverts, S. H. Muller, and C. A. J. Ammerlaan, Phys. Rev. B **18**, 6834 (1978).
[20]G. D. Watkins and J. W. Corbett, Phys. Rev. **138**, A543 (1965).
[21]M. G. Ganchenkova, L. E. Oikkonen, V. A. Borodin, S. Nicolaysen, and R. M. Nieminen, Mater. Sci. Eng. B **159**, 107 (2009).
[22]G. D. Watkins, Physica B **376**, 50 (2006).
[23]J. I. Iwata, K. Shiraishi, and A. Oshiyama, Phys. Rev. B **77**, 115208 (2008).
[24]D. V. Makhov and L. J. Lewis, Phys. Rev. B **72**, 073306 (2005).
[25]R. R. Wixom and A. F. Wright, Phys. Rev. B **74**, 205208 (2006).
[26]Z. F. Di, Y. Q. Wang, M. Nastasi, L. Shao, J. K. Lee, and N. D. Theodore, Appl. Phys. Lett. **93**, 104103 (2008).
[27]B. B. Nielsen, L. Hoffmann, and M. Budde, Mater. Sci. Eng. B **36**, 259 (1996).
[28]N. Rochat, A. Tauzin, F. Mazen, and L. Clavelier, Electrochem. Solid-State Lett. **13**, G40 (2010).
[29]W. Düngen, R. Job, Y. Ma, Y. L. Huang, T. Mueller, W. R. Fahrner, L. O. Keller, J. T. Horstmann, and H. Fiedler, J. Appl. Phys. **100**, 034911 (2006).
[30]E. V. Lavrov, J. Weber, L. Huang, and B. B. Nielsen, Phys. Rev. B **64**, 035204 (2001).
[31]M. Fehr, A. Schnegg, B. Rech, K. Lips, O. Asthakov, F. Finger, G. Pfanner, C. Freysoldt, J. Neugebauer, R. Bittl, and C. Teutloff, Phys. Rev. B **84**, 245203 (2011).
[32]M. Stutzmann and D. K. Biegelsen, Phys. Rev. B **40**, 9834 (1989).
[33]T. Umeda, S. Yamasaki, J. Isoya, and K. Tanaka, Phys. Rev. B **59**, 4849 (1999).
[34]P. Giannozzi, S. Baroni, N. Bonini, M. Calandra, R. Car, C. Cavazzoni, D. Ceresoli, G. L. Chiarotti, M. Cococcioni, I. Dabo, A. Dal Corso, S. de Gironcoli, S. Fabris, G. Fratesi, R. Gebauer, U. Gerstmann, C. Gougoussis, A. Kokalj, M. Lazzeri, L. Martin-Samos, N. Marzari, F. Mauri, R. Mazzarello, S. Paolini, A. Pasquarello, L. Paulatto, C. Sbraccia, S. Scandolo, G. Sclauzero, A. P. Seitsonen, A. Smogunov, P. Umari, and R. M. Wentzcovitch, J. Phys.: Condens. Matter **21**, 395502 (2009).
[35]J. P. Perdew, K. Burke, and M. Ernzerhof, Phys. Rev. Lett. **77**, 3865 (1996).
[36]The GIPAW-reconstruction data for the all-electron wave function has been generated by Ari P. Seitsonen.
[37]S. Blügel, H. Akai, R. Zeller, and P. H. Dederichs, Phys. Rev. B **35**, 3271 (1987).
[38]R. H. Luchsinger, Y. Zhou, and P. F. Meier, Phys. Rev. B **55**, 6927 (1997).
[39]H. J. Monkhorst and J. D. Pack, Phys. Rev. B **13**, 5188 (1976).
[40]M. J. Frisch, G. W. Trucks, H. B. Schlegel, G. E. Scuseria, M. A. Robb, J. R. Cheeseman Jr., J. A. Montgomery, T. Vreven, K. N. Kudin, J. C. Burant, J. M. Millam, S. S. Iyengar, J. Tomasi, V. Barone, B. Mennucci, M. Cossi, G. Scalmani, N. Rega, G. A. Petersson, H. Nakatsuji, M. Hada, M. Ehara, K. Toyota, R. Fukuda, J. Hasegawa, M. Ishida, T. Nakajima, Y. Honda, O. Kitao, H. Nakai, M. Klene, X. Li, J. E. Knox, H. P. Hratchian, J. B. Cross, V. Bakken, C. Adamo, J. Jaramillo, R. Gomperts, R. E. Stratmann, O. Yazyev, A. J. Austin, R. Cammi, C. Pomelli, J. W. Ochterski, P. Y. Ayala, K. Morokuma, G. A. Voth, P. Salvador, J. J. Dannenberg, V. G. Zakrzewski, S. Dapprich, A. D. Daniels, M. C. Strain, O. Farkas, D. K. Malick, A. D. Rabuck, K. Raghavachari, J. B. Foresman, J. V. Ortiz, Q. Cui, A. G. Baboul, S. Clifford, J. Cioslowski, B. B. Stefanov, G. Liu, A. Liashenko, P. Piskorz, I. Komaromi, R. L. Martin, D. J. Fox, T. Keith, M. A. Al-Laham, C. Y. Peng, A. Nanayakkara, M. Challacombe, P. M. W. Gill, B. Johnson, W. Chen, M. W. Wong, C. Gonzalez, and J. A. Pople, Gaussian 03, Revision D.01, Gaussian, Inc., Wallingford, CT (2004).
[41]G. Pfanner, C. Freysoldt, and J. Neugebauer, Phys. Rev. B **83**, 144110 (2011).
[42]J. Coutinho, R. Jones, P. R. Briddon, and S. Öberg, Phys. Rev. B **62**, 10824 (2000).
[43]P. Johannesen, B. B. Nielsen, and J. R. Byberg, Phys. Rev. B **61**, 4659 (2000).
[44]F. Corsetti and A. A. Mostofi, Phys. Rev. B **84**, 035209 (2011).
[45]A. F. Wright, Phys. Rev. B **74**, 165116 (2006).
[46]U. Gerstmann, M. Rohrmüller, F. Mauri, and W. G. Schmidt, Phys. Status Solidi C **7**, 157 (2010).
[47]H. Xu, Phys. Rev. B **46**, 1403 (1992).
[48]P. Stallinga, P. Johannesen, S. Herstrøm, K. B. Nielsen, B. B. Nielsen, and J. R. Byberg, Phys. Rev. B **58**, 3842 (1998).
[49]To check that this is not caused by structural effects, we have also computed the a-parameter with the PBE functional for the structure obtained by LDA. The corresponding result is in better agreement (on the order of 50%) with a true PBE calculation as well as experiment. Thus we conclude that the improvement in accuracy is directly related to the PBE functional.
[50]D. K. Biegelsen and M. Stutzmann, Phys. Rev. B **33**, 3006 (1986).